BRIEF COMMUNICATION

Kinetics of the orientation transition in the lyotropic lamellar phase

Shuji Fujii*, Yuki Yamamoto

Department of Materials Science and Technology, Nagaoka University of Technology, Niigata, Nagaoka 940-2188, Japan

Abstract   Kinetics of the orientation transition in the triblock copolymer lamellar phase is studied by viscometry. We find that the strain-controlled mechanism dominates the transition kinetics. We propose a possible scenario of the orientation transition from the viewpoint of the dislocation dynamics. We could also evaluate the critical shear rate of the orientation transition by assuming the limiting velocity of the dislocations under shear. Evaluated value is in good agreement with the experimental observation. The nucleation of the dislocations might be necessary for the orientation transition.

Keywords   lamellar phase, orientation transition, non-equilibrium transition, dislocation, rheology

1. Introduction

Rheology of the lamellar phase has many open issues such as a defect-mediated shear-thinning behavior, the origin of the elasticity, and the non-equilibrium structural transition induced by shear [1–11]. Especially the non-equilibrium structural transition has been extensively studied both experimentally and theoretically for more than two decades. It is known that the lyotropic lamellar phase shows two non-equilibrium structural transitions. One is a thermodynamically stable multilamellar vesicle (MLV) phase formation under shear flow [1–5]. And another one is an orientation transition of the lamellae from parallel to perpendicular orientation [5–7, 12–17]. Since there are many reports on the orientation transition for many systems such as thermotropic smectic phase, amphiphilic lamellar phase, and block copolymer melt [18–21], the orientation transition is likely to be an universal structural transition in the layered system. Nonetheless, in contrast to the MLV formation mechanism which has generated a lot of interests in understanding, the orientation transition mechanism still

remains speculative. And also there is no experimental report on the transition kinetics except for molecular dynamics simulation [17]. For clear understanding of the non-equilibrium structural transition, kinetic pathway in particular is important to address discrepancy from the MLV formation mechanism.

In general, the undulation fluctuation is responsible for the stability of the lamellar phase in the thermal equilibrium state, since it yields repulsive Helfrich interaction between lamellae [22]. Theoretical studies expect that the lamellar will lose its stability as the shear rate gradually increases because of suppression of the undulation fluctuation [12–16]. Therefore the reduced repulsive force generates effective dilation along the layer normal of the lamellae in order to retain the equilibrium layer spacing. This is the undulation instability. As the dilation becomes larger than the critical value, coherent buckling of the lamellae sets in along the neutral direction, and the orientation transition is eventually triggered. However, we should also note that such dilation creates dislocations, which significantly affect the rheological properties of the lamellar phase [9–11]. In addition, many dislocations accumulate into a texture known as a focal conic domain (FCD) which also affects the rheology [23–25]. Indeed, the rheological properties of the lamellar phase is closely related to the structural response such as the dynamic orientation state, a motion of dislocations and a coarsening of the defect [4, 6, 7, 26]. Therefore, in order to understand the orientation transition of the lamellar phase, we need to consider all contributions of the undulation flucuation, the nucleation of the dislocations, and their assembly into defects.

In this brief communication, we present transient viscosity data associated with the orientation transition. To our knowledge, this is the first experimental study on the kinetics of the orientation transition. In the following section, the sample and experimental method are shortly described. Then, the experimental results of the transient behavior are presented when the shear rate is changed from parallel to perpendicular lamellae and vice versa. We also discuss the

---

*E-mail: sfujii@mst.nagaokaut.ac.jp

possible mechanism of the orientation transition and the origin of the critical shear rate. Finally main findings in this study are summarized in the conclusion.

2. Sample and Viscometry

We used ternary lyotropic lamellar phase composed of amphiphilic triblock copolymers, Butanol and distilled water. The amphiphilic triblock copolymer, trade name of Pluronic P123, obtained from BASF was used as received. This triblock copolymer consists of two hydrophilic ethylene oxide, EO, blocks bounded to a central hydrophobic propylene oxide, PO, block. A degree of polymerization of hydrophilic EO block is $N_{EO} \approx 23$. And the degree of polymerization of PO chains of $N_{PO} \approx 59$. The prescribed amount of block copolymer and Butanol were dissolved into the distilled water H_2O and gently stirred by a magnetic stirrer for 2 days. Pluronic P123 concentration was fixed at 23 wt% and solvent composition, the ratio of butanol against the water was fixed at 0.3. Butanol plays a role of a cosurfactant and thus most of butanol is located in the interface between hydrophilic and hydrophobic parts [3]. In all the measurements, sample was always cooled down until the lamellar phase undergoes transition into an isotropic phase with low viscosity. And then the sample in the isotropic phase was loaded on the sample cell. Then temperature was set to the measurement condition $T = 23°C$ and we waited for 1200 s. Shear jump and quench experiments were performed using an ARES-G2 strain-controlled rheometer of TA Instrument Co., Ltd., with a couette geometry (hight of bob; 13 mm, gap size; 250 μm). In the kinetic experiments, initial shear rate $\dot{\gamma}_i$ was applied to the sample until the steady state is obtained. When the viscosity reached to the steady value, the shear rate was changed to final shear rate $\dot{\gamma}_f$ in a manner of the step function. In the

ARES-G2 with the couette shear cell, the shear rate reached to the fixed value after 0.05 s.

Small angle X-ray scattering (Rheo-SAXS) measurement was carried out using synchrotron radiation at beam line BL-10C of the Photon Factory at the Institute of Materials Structure Science of the High Energy Accelerator Research Organization in Tsukuba, Japan [27]. Self-made shear cell with the couette geometry was equipped on the beam line. In the rheo-SAXS measurements, 2D scattering patterns in neutral n-velocity v plane and neutral n-velocity gradient ∇v plane are obtained.

3. Dynamic orientation state

Steady state viscosity and SAXS patterns are shown in Fig. 1. The system shows a shear-thinning behavior with a power law relation of $\eta \sim \dot{\gamma}^{-1/3}$, which has a theoretically predicted exponent by Lu *et al.* [11]. The shear-thinning is followed by a shift into the Newtonian like behavior. In the SAXS patterns, at lower shear rates $\dot{\gamma} = 30$ and 50 s^{-1}, the Bragg peak can be observed along the neutral n direction in the v-n plane and along the velocity gradient ∇v direction in ∇v-n plane. This is indicative of the parallel oriented lamellar phase, so-called c-orientation [3, 6, 28, 29]. On the other hand, at higher shear rates $\dot{\gamma} = 100$ and 300 s^{-1}, secondary Bragg peak appears along n direction in the v-n plane. In addition, the Bragg peak position in the ∇v-n plane turns by 90° and appears along n direction. This is a typical pattern for the perpendicularly oriented lamellar phase, a-orientation [3, 6, 28, 29]. Thus, the shear-thinning and the Newtonian like behavior are assigned to the lamellar phase with c and a-orientation, respectively. In this system, there seems be a critical shear rate of the orientation transition between $\dot{\gamma} = 50$ and 70 s^{-1}. We should note that the critical shear rate is sensitive to the sample prepara-
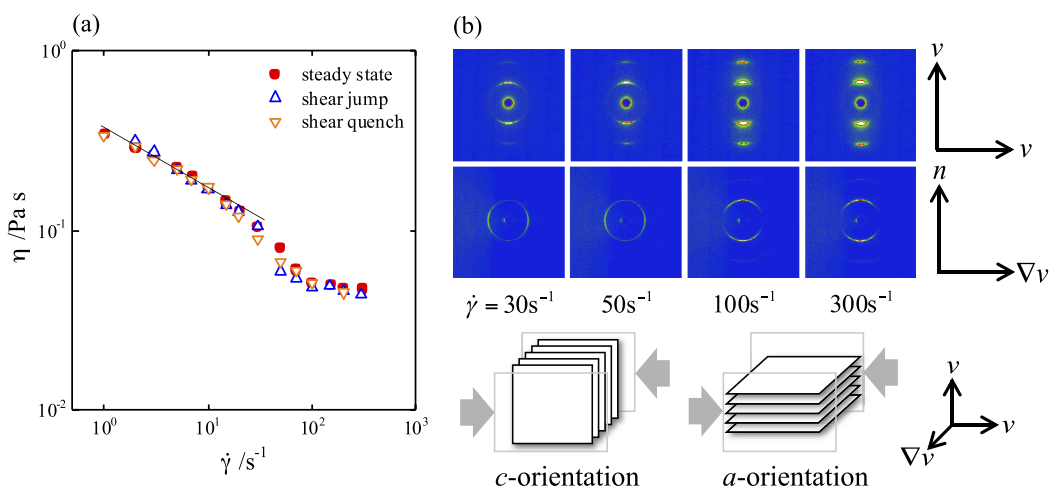
Fig. 1 (a): Steady shear viscosity as a function of shear rate. Solid line shows the power law relation $\eta \sim \dot{\gamma}^{-1/3}$ of the shear-thinning behavior. For the reference, steady state viscosity obtained after the shear jump and quench are also shown. (b): Typical SAXS patterns obtained from different scattering plane, upper line; neutral n-velocity v plane and bottom line; neutral n-velocity gradient ∇v plane. Schematic diagrams of the lamellar phase with c and a-orientation are also shown.

tion. Depending on the sample preparation, the perpendicular lamellar phase is observed at $\dot{\gamma} = 50 \text{ s}^{-1}$.

On the basis of the viscometry and SAXS data, we performed transient viscosity measurements by shear jump or quench across the critical shear rate. In the shear jump experiment, the shear rate was jumped up from initial value $\dot{\gamma}_i = 1 \text{ s}^{-1}$ to different final values $\dot{\gamma}_f$. On the other hand, in the shear quench experiment, the shear rate was quenched from $\dot{\gamma}_i = 300 \text{ s}^{-1}$ to different $\dot{\gamma}_f$. Steady state viscosity reached after the shear jump and quench are compared with each other in Fig. 1. Each steady state viscosities are consistent.

4. Shear jump experiments

Transient behavior of the viscosity after the shear jump from c-orientation at $\dot{\gamma}_i = 1 \text{ s}^{-1}$ to different $\dot{\gamma}_f$ is shown in Fig. 2. When the shear rate was jumped between the lamellar phases with c-orientation, the viscosity instantaneously dropped at short time and gradually increased and reached to the steady state with time. As the shear rate is increased, slight overshoot appeared at $\dot{\gamma} = 20$ and 30 s^{-1}. In the figure, we show only viscosity growth because the drop of the viscosity at short time range could not be detected with enough accuracy. On the other hand, when the shear rate was jumped up into a-orientation, the viscosity showed a multi step behavior; the overshoot at short time range followed by thixotropic behavior with shoulder. Transient behavior significantly depends on whether $\dot{\gamma}_f$ belongs to c-orientation or a-orientation. Multi step relaxation indicates the contribution of several modes with different time scales. In order to estimate the time scale of the kinetics, we defined a characteristic time of the viscosity growth t_g at

lower shear rates by an intersection point between two lines. In the vicinity of the orientation transition, a peak position of the overshoot indicated by arrows was picked up as the characteristic time. We also defined two characteristic times in the orientation transition by the maximum position of the viscosity t_m and shoulder where two lines intersect t_{th} as indicated by arrows. As $\dot{\gamma}_f$ is increased, t_{th} in the orientation transition gradually disappeared. Above $\dot{\gamma}_f \geq 200 \text{ s}^{-1}$, we could not extract t_{th}.

Extracted characteristic times are plotted as a function of $\dot{\gamma}_f$ in Fig. 2(b). These characteristic times for the viscosity growth and orientation transition are inversely proportional to $\dot{\gamma}_f$. It indicates that the kinetics of the orientation transition is driven by a strain-controlled mechanism. These characteristic times are respectively well scaled by strain, $\dot{\gamma}_f t_g \simeq 300$, $\dot{\gamma}_f t_m \simeq 100$ and $\dot{\gamma}_f t_{th} \simeq 2000$.

The shear-thinning behavior of the lamellar phase is significantly mediated by the nucleation-annihilation dynamics of the dislocations [11]. The nucleation arises from the undulation instability, and the annihilation occurs through the collision and reconnection of separated dislocations. The power law relation of the steady state viscosity $\eta \sim \dot{\gamma}^{-1/3}$ with the theoretically predicted exponent indicates the domination of the nucleation-annihilation dynamics. In this model, the nucleation-annihilation dynamics takes place at a frequency proportional to $\dot{\gamma}$. The viscosity growth may be thus induced by the increase of the dislocation density ρ in order to accommodate the system to different non-equilibrium state. Nucleation of the dislocations by shearing has been visually observed in some layered systems [7, 24, 30]. However, in this study, we could not see the dislocations and meso-scale structural changes under the optical microscope due to the resolution limitation [29]. Scaling of each transient curve by the strain
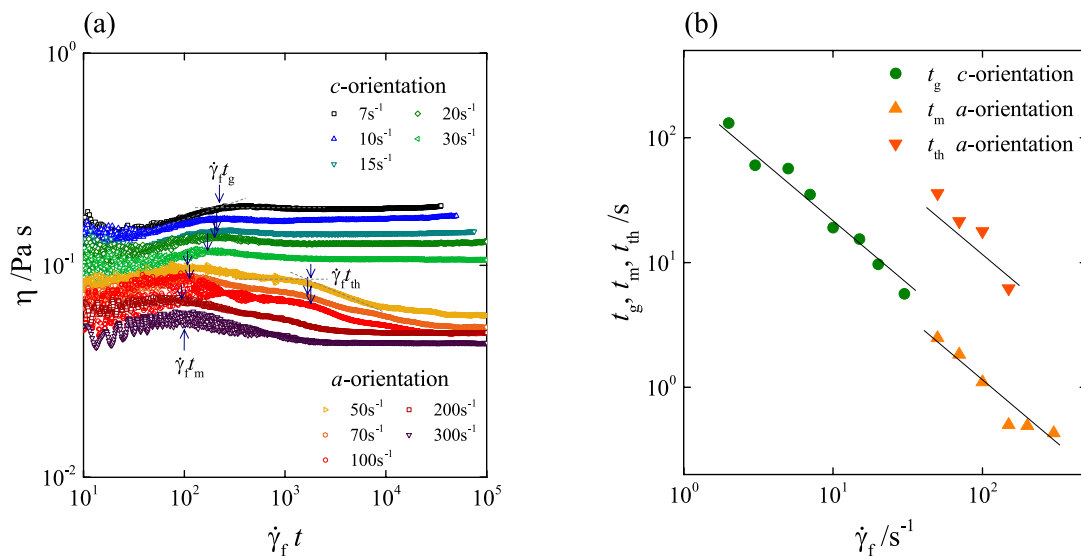
Fig. 2 (a): Transient viscosity after the shear jump from $\dot{\gamma}_i = 1 \text{ s}^{-1}$ to different $\dot{\gamma}_f$. Transient curves are plotted as a function of accumulated strain $\dot{\gamma}_f t$. Each symbols correspond to the different $\dot{\gamma}_f$. In the orientation transition, we extract two characteristic times, t_m where the viscosity shows the maximum value and t_{th} at the shoulder. Small arrows show the characteristic times t_g, t_m and t_{th}. (b): Characteristic times t_g, t_m and t_{th} as a function of $\dot{\gamma}_f$. Solid lines are the power law relation with a slope of -1, $t \sim \dot{\gamma}_f^{-1}$.

proposes that a production rate of dislocations, $\Delta\rho/\Delta t$, is proportional to $\dot{\gamma}_f$, and the accommodation to a new steady state is achieved after a specific strain. Characteristic time t_g may be thus assigned to the production of the dislocations. Here we should note that the overshoot of the viscosity at $\dot{\gamma}_f$ = 30 s^{-1} shifted to lower strain in Fig. 2(a). Characteristic time t_g thus slightly deviates from the inverse-proportionality as the critical shear rate is reached. Close to the orientation transition, the dislocations may be produced quickly compared to the shear-thinning region described by the power law relation.

In the orientation transition behavior, on the other hand, thixotropic behavior with the shoulder will be attributed to the alignment of the lamellar in a-orientation. We argue the orientation mechanism in a later section.

5. Shear quench experiments

Fig. 3(a) shows a shear quench behavior from a-orientation at $\dot{\gamma}_i$ = 300 s^{-1} to different $\dot{\gamma}_f$. At $\dot{\gamma}_f$ = 70 and 100 s^{-1} corresponding to a-orientation, the transient viscosity showed no remarkable time development. Shear rate quench between the same orientations does not yield specific relaxation behavior since the reorganization of the lamellar orientation does not occur. When the shear rate was quenched into c-orientation region, on the other hand, the viscosity increased with time as the orientation of lamellae recovers from a to c-orientation. In the vicinity of the critical shear rate $\dot{\gamma}_c \simeq 50$ s^{-1}, the viscosity slightly increased and reached to the steady state. As $\dot{\gamma}_f$ departed from the critical shear rate into low shear rate, the viscosity growth became remarkable. In the recovery process, the viscosity showed a peak followed by the steady state.

The viscosity in the recovery process was fitted with following compressed exponential relation in order to extract a characteristic recovery time τ, $\eta \simeq A \exp (\tau/t)^\beta$ with compressed exponent $\beta \geq 1$. Here, A is a pre-factor. Simple compressed exponential relation well fits the recovery process. Extracted recovery time τ and characteristic time t_{peak} at the viscosity peak are summarized as a function of $\dot{\gamma}_f$ in Fig. 3(b). As $\dot{\gamma}_f$ is decreased, these two characteristic times gradually approach to a power law relation with a slope of −1. Compressed exponent value β scatters around β = 1.5. Inverse proportionality of τ and t_{peak} against $\dot{\gamma}_f$ indicates that lamellar reorientation mechanism from a to c-orientation is also dominated by a strain-controlled mechanism as well as the orientation transition. We note that the disintegration of the MLV structure into the lamellar phase with c-orientation observed after the shear quench also follows the strain controlled process [31].

Recovery process from a to c-orientation reveals specific relaxation modes associated with the motion of the dislocations and their assembly. In our recent study on the shear quench behavior of the thermotropic smectic phase, we found three relaxation modes, the first one corresponding to the climb motion of the dislocation, the second one to the FCD formation, and the third to assembly of the oily streak according to the realignment of the FCDs in series along the flow direction [32]. The characteristic time τ is rather closer to the time scale of the the oily streak arrangement $\tau \sim 10^2$–10^3 s. Indeed, the time scales of the climb motion and FCD formation are much shorter than τ [33]. The lamellar phase with c-orientation in this study includes the oily streaks with high density [29]. Therefore, it is plausible to attribute the characteristic time τ to the alignment of FCDs forming oily streak.
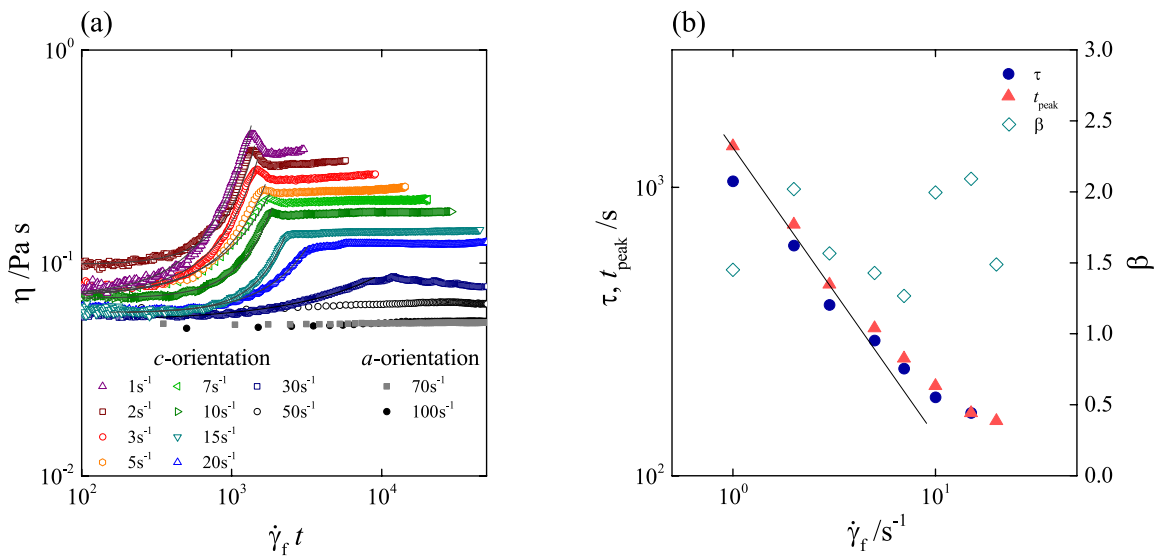
Fig. 3 (a): Transient viscosity after the shear quench from $\dot{\gamma}_i$ = 300 s^{-1} to different $\dot{\gamma}_f$. Each symbols correspond to $\dot{\gamma}_f$. Solid curves show the best fit to the compressed exponential function with the single relaxation time. (b): Extracted relaxation time τ, peak time t_{peak}, and compressed exponent β as a function of $\dot{\gamma}_f$. Solid lines are the power law relation with the slope of −1, $\tau \sim \dot{\gamma}_f^{-1}$.
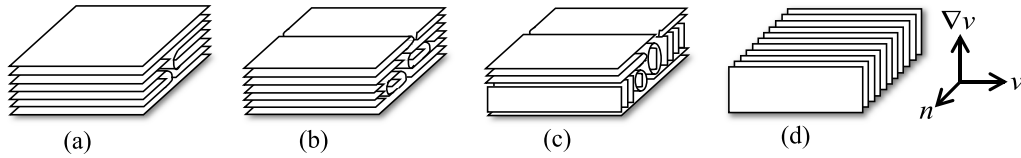
Fig. 4 Schematic diagram of the lamellar flipping scenario from c to a-orientation after the shear jump. (a): Initial state at $\dot{\gamma}_i$. (b): After the shear jump, dislocations are nucleated and lamellae are disassembled into small domains which allows the rotation into a-orientation at t_m. (c): Most of fragmented domains rotate into a-orientation at t_{th}. (d): Well-aligned lamellar with a-orientation is formed by the annihilation of dislocations in the long-time tail.

6. Mechanism of the orientation transition

6.1. Kinetic pathway of the orientation transition

In this section, we propose the possible scenario of the orientation transition on the basis of the molecular dynamics simulation study by Guo [17]. In the simulation, the undulation fluctuation along the flow direction was suppressed by shear. Since the undulation fluctuation along the neutral direction is not coupled to the shear flow, lamellae break up into mono-domains along the neutral direction. The fragmented lamellar domain then rotates into the perpendicular orientation and organizes the perpendicularly oriented lamellar phase by migration and annihilation of the defects. Because of the drastic realignment of the lamellae, the viscosity drops significantly after the fragmentation. Then, the viscosity slowly decreases with time because of the slow kinetics of the migration and annihilation of dislocations.

Transient behavior with multi modes in Fig. 2(a) is qualitatively similar to the simulation. Possible lamellar flipping scenario is schematically summarized in Fig. 4. Characteristic time t_m at the maximum viscosity may correspond to the beginning of the fragmentation of the lamellar. After the fragmentation, the lamellar mono-domains rotate and start to merge at $\dot{\gamma}_f t_{th} \simeq 2000$. Long-time tail after $\dot{\gamma}_f t_{th}$ may thus be attributed to the annihilation of dislocations to form aligned lamellar mono-domain with a-orientation. Above scenario proposed on the basis of the simulation result is still too much speculative, because of the lack of the experimental information on the time development of the structure. For further investigation, it is necessary to measure the time-resolved rheo-SAXS with high temporal resolution.

It is surprising that both of orientation transition behavior from c to a-orientation and vice versa can be reduced by the strain. Appearance of the shoulder at fixed strain indicates that a flip rate of the lamellar domains $\Delta\theta/\Delta t$ is also proportional to the shear rate. Here θ is an inclination angle of the lamellar domains. Experimental finding on the scaling behavior suggests that the nucleation of the defects, the rotation of the lamellar domain, and the annihilation of the dislocations are driven by the strain-controlled mechanism.

6.2. Origin of the critical shear rate

Finally we discuss the origin of the critical shear rate. As can be seen in Fig. 3, the time for the arrangement of the oily streaks asymptotically approaches to a certain value as $\dot{\gamma}_f$ is increased. The oily streak arrangement taking place with constant τ indicates that there is a limiting velocity of the dislocation at high $\dot{\gamma}_f$. Motion of the dislocations depends on their inherent mobility M. At low $\dot{\gamma}_f$, the dislocations are able to move with the flow [34], and the oily streak formation will occur gradually. In contrast, at high $\dot{\gamma}_f$, the dislocations are no longer able to follow the flow. At this limit, the dilation will develop around the dislocations, which lead to rapid creation of the oily streaks independently of $\dot{\gamma}_f$. In other words, once the shear rate exceeds over the limiting velocity, excess formation of the dislocations will destabilize the lamellar phase because of inhomogeneous lamellar spacing around the dislocations. In order to keep the lamellar spacing constant, the system forms a-orientation to be able to flow, since the orientational order and lamellar spacing are not disturbed in a-orientation. This limiting velocity of the dislocation may correspond to the critical shear rate of the orientation transition.

On the basis of our assumption on the limiting velocity of the dislocations, we simply estimate the critical shear rate. The mobility of the dislocation M is evaluated by a relation of $M \sim 4\pi^2 b/\eta$ with a Burgers vector b and viscosity of the lamellar [35]. FCDs in the oily streak of the lyotropic lamellar phase in general has the length of the major ellipse axis of $a \sim 10$ μm [29]. In order to form FCDs with the size of $a \sim 10$ μm, the Burgers vector of the defects will be a few μm [23]. Using experimental value of the viscosity at the critical shear rate, $\eta \simeq 0.06$ Pa s, the mobility at the limit can be estimated to be $M \sim 10^{-5}$ m^2 s kg^{-1}. The velocity of the dislocation at the limit is further given by the mobility M and the shear stress at the critical shear rate, $v_{lim} = M\sigma$ [36]. The critical shear rate is evaluated by dividing the limiting velocity with the sample thickness (250 μm). Then the critical shear rate is estimated to be $\dot{\gamma}_{lim} \sim 10^1$–$10^2$ s^{-1}, which is in good agreement with our experimental value.

In several models developed by considering the suppression of the undulation fluctuation under shear, the critical shear rate is estimated to be $\dot{\gamma}_c \sim k_B T/\eta d^3$, in wide range of the lamellar spacing d [12, 15, 16]. However, the critical shear rate in these models ($\sim 10^4$ s^{-1}) does not agree with the

experimental value in this study even if the steady state viscosity is incorporated instead of the solvent viscosity. Here, the lamellar spacing d in this system is 18 nm. Agreement of the critical shear rate roughly estimated via the limiting velocity suggests that the nucleation of dislocations is necessary condition, while the presence of too many defects will invalidate the layer suppression effects. The orientation transition in the lamellar phase with many defects may belong to different class from the undulation fluctuation dominated system such as the dilute lamellar phase with less dislocations.

7. Conclusion

We have focused on the kinetics of the orientation transition of the lyotropic lamellar phase. We proposed a speculative scenario of the orientation transition. First, the nucleation of the dislocations enables the fragmentation into small lamellar domains which can rotate to a-orientation in order to keep the lamellar spacing constant. Then well-aligned lamellar phase with a-orientation is eventually achieved by annihilation of the fragmented lamellar domains.

Experimental finding on the scaling behavior of the transient viscosity indicates that the strain-controlled mechanism dominates the transition kinetics. Interestingly, we also found that the recovery process from a-orientation also follows the strain-controlled mechanism. Good agreement of the critical shear rate roughly evaluated from the limiting velocity of the dislocation proposes that the orientation transition in this system may necessitate the nucleation of dislocations. The defect dynamics could be responsible not only for the rheological behavior but also for the non-equilibrium structural transition.

References

1. Diat O, Roux D, Nallet F. Effect of shear on a lyotropic lamellar phase. J Phys II France. 1993; 3: 1427–1452.
2. Roux D, Nallet F, Diat O. Rheology of lyotropic lamellar phase. EPL. 1993; 24: 53–58.
3. Zipfel J, Berghausen J, Schmidt G, Lindner P, Alexandridis P, Richtering W. Influence of shear on solvated amphiphilic block copolymers with lamellar morphology. Macromol. 2002; 35: 4046–4074.
4. Fujii S, Mitsumasu D, Isono Y, Richtering W. Shear-induced onion formation of polymer-grafted lamellar phase. Soft Matter. 2012; 8: 5381–5390.
5. Berghausen J, Zipfel J, Lindner P, Richtering W. Influence of water soluble polymers on the shear-induced structure formation in lyotropic lamellar phase. J Phys Chem B. 2001; 105: 11081–11088.
6. Panizza P, Archambault P, Roux D. Effects of shear on the smectic. A phase of thermotropic liquid crystals. J Phys II France. 1995; 5: 303–311.
7. Fujii S, Ishii Y, Komura S, Lu CYD. Smectic rheology close to the smectic-nematic transition. EPL. 2010; 90: 64001.
8. Dhez O, Nallet F, Diat O. Influence of screw dislocations on the orientation of a sheared lamellar phase. EPL. 2010; 55: 821–826.
9. Meyer C, Asnacios S, Bourgaux C, Kleman M. Rheology of lyotropic and thermotropic lamellar phase. Rheol Acta. 2000; 39: 223–233.
10. Meyer C, Asnacios S, Kleman M. Universal properties of lamellar systems under weak shear. Eur Phys J E. 2001; 6: 245–253.
11. Lu C-YD, Chen P, Ishii Y, Komura S, Kato T. Non-linear rheology of lamellar liquid crystals. Eur Phys J E. 2008; 25: 91–101.
12. Ramaswamy S. Shear-induced collapse of the dilute lamellar phase. Phys Rev Lett. 1992; 69: 112–115.
13. Bruinsma R, Rabin Y. Shear-flow enhancement and suppression of fluctuations in smectic liquid crystals. Phys Rev A. 1992; 45: 994–1008.
14. Auernhammer G K, Brand HR, Pleiner H. Shear-induced instabilities in layered liquids. Phys Rev E. 2002; 66: 061707.
15. Marlow SW, Olmsted PD. The effect of shear flow on the Helfrich interaction in lyotropic lamellar systems. Eur Phys J E. 2002; 8: 485–497.
16. Al khawaji A, Kellay H. Observations of the collapse of dilute lyotropic lamellar phases under shear flow. Phys Rev Lett. 2000; 84: 3073–3076.
17. Guo H. Shear-induced parallel-to-perpendicular orientation transition in the amphiphilic lamellar phase: a nonequilibrium molecular-dynamics simulation study. J Chem Phys. 2006; 124: 054902.
18. Koppi KA, Tirrell M, Bates FS, Almdaland K, Colby RH. Lamellae orientation in dynamically sheared diblock copolymer melts. J Phys II. 1992; 2: 1941–1959.
19. Fredrickson GH, Bates FS. Dynamics of block copolymers: theory and experiment. Annu Rev Mater Sci. 1996; 26: 501–550.
20. Wiesner U. Lamellar diblock copolymers under large amplitude oscillatory shear flow: Order and dynamics. Macromol Chem Phys. 1997; 198: 3319–3352.
21. Chen Z-R, Kornfield JA. Flow-induced alignment of lamellar block copolymer melts. Polymer. 1998; 39: 4679–4699.
22. Helfrich W. Steric interactions of fluid membranes in multilayer systems. Z Naturforsch. 1978; 33a: 305.
23. Boltenhagen P, Lavrentvich O, Kleman M. Oily streaks and focal conic domains in L_a lyotropic liquid crystals. J Phys II France. 1991; 1: 1233–1252.
24. Horn RG, Kleman M. Observations on shear-induced textures and rheology of a smectic-A phase. Ann Phys. 1978; 3: 229–234.
25. Fujii S, Komura S, Ishii Y, Lu C-YD. Elasticity of smectic liquid crystals with focal conic domains. J Phys Cond Matt. 2011; 23: 235105.
26. Fujii S, Komura S, Lu CYD. Structural rheology of the smectic phase. Materials. 2014; 7: 5146.
27. Ueki T, Hiragi Y, Kataoka M, Inoko Y, Amemiya Y, Izumi Y, Tagawa H, Muroga Y. Aggregation of bovine serum albumin upon cleavage of its disulfide bonds, studied by the time-resolved small-angle x-ray scattering technique with synchrotron radiation. Bio Phys Chem. 1985; 23: 115–124.
28. Fujii S, Yamamoto Y. Orientation transition of defective lyotropic triblock copolymer lamellar phase. J Biorheol. 2014; 28: 55–60.
29. Fujii S, Yamamoto Y. Dynamic orientation transition of the lyotropic lamellar phase at high shear rate. Accepted in Soft Matter. 2015; DOI: 10.1039/c5sm01755f.
30. Winey KI, Patel SS, Larson RG, Watanabe H. Interdependence of shear deformations and block copolymer morphology. Macromol.

1993; 26: 2542–2549.

31. Fujii S, Richtering W. Shear quench-induced disintegration of nonionic surfactant C10E3 onion phase. Soft Matter. 2013; 9: 5391–5400.

32. Fujii S, Komura S, Lu C-YD. Structural rheology of focal conic domains: a stress-quench experiment. Soft Matter. 2014; 10: 5289–5295.

33. de Gennes PG, Prost J. The Physics of Liquid Crystals. Carendon Press: London; 1993.

34. Oswald P, Kleman M. Lubrication theory of smectic A phases. J Phys (Paris) Lett. 1982; 43: L-411.

35. Pleiner H. Dynamics of a screw dislocation in smectic A liquid crystals. Philos Mag A. 1986; 54: 421–439.

36. Peach K, Koehler J. The forces exerted on dislocations and the stress fields produced by them. Phys Rev. 1950; 80: 436–439.